Available online at www.sciencedirect.com
ScienceDirect
Biochimica et Biophysica Acta 1768 (2007) 3116–3126
Biochimica et Biophysica Acta
BBA
www.elsevier.com/locate/bbamem

Review

NMR structural studies of the antibiotic lipopeptide daptomycin in DHPC micelles

Walter R.P. Scott [a], Seung-Bin Baek [a], David Jung [b], Robert E.W. Hancock [b], Suzana K. Straus [a,*]

[a] *Department of Chemistry, University of British Columbia, 2036 Main Mall, Vancouver, BC, Canada V6T 1Z1*
[b] *Department of Microbiology and Immunology, University of British Columbia, 232B -2259 Lower Mall, Vancouver, BC, Canada V6T 1Z4*

Received 30 June 2007; received in revised form 30 August 2007; accepted 31 August 2007
Available online 15 September 2007

Abstract

Daptomycin is a cyclic anionic lipopeptide that exerts its rapid bactericidal effect by perturbing the bacterial cell membrane, a mode of action different from most other currently commercially available antibiotics (except e.g. polymyxin and gramicidin). Recent work has shown that daptomycin requires calcium in the form of Ca^{2+} to form a micellar structure in solution and to bind to bacterial model membranes. This evidence sheds light on the initial steps in the mechanism of action of this novel antibiotic. To understand how daptomycin goes on to perturb bacterial membranes, its three-dimensional structure has been determined in the presence of 1,2-dihexanoyl-*sn*-glycero-3-phosphocholine (DHPC) micelles. NMR spectra of daptomycin in DHPC were obtained under two conditions, namely in the presence of Ca^{2+} as used by Jung et al. [D. Jung, A. Rozek, M. Okon, R.E.W. Hancock, Structural transitions as determinants of the action of the calcium-dependent antibiotic daptomycin, Chem. Biol. 11 (2004) 949–57] to solve the calcium-conjugated structure of daptomycin in solution and in a phosphate buffer as used by Rotondi and Gierasch [K.S. Rotondi, L.M. Gierasch, A well-defined amphipathic conformation for the calcium-free cyclic lipopeptide antibiotic, daptomycin, in aqueous solution, Biopolymers 80 (2005) 374–85] to solve the structure of apo-daptomycin. The structures were calculated using molecular dynamics time-averaged refinement. The different sample conditions used to obtain the NMR spectra are discussed in light of fluorescence data, lipid flip-flop and calcein release assays in PC liposomes, in the presence and absence of Ca^{2+} [D. Jung, A. Rozek, M. Okon, R.E.W. Hancock, Structural transitions as determinants of the action of the calcium–dependent antibiotic daptomycin, Chem. Biol. 11 (2004) 949–57]. The implications of these results for the membrane perturbation mechanism of daptomycin are discussed.

Keywords: Daptomycin; Lipopeptide; Solution state NMR; NOEs; Structure calculation; Mechanism of action

Contents

1. Introduction

In recent years, significant advances in both solution and solid state NMR have led to an ever increasing number of membrane peptide and protein structure and dynamics studies

* Corresponding author. Tel.: +1 604 822 2537; fax: +1 604 822 2157.
E-mail address: sstraus@chem.ubc.ca (S.K. Straus).

0005-2736/$ - see front matter © 2007 Elsevier B.V. All rights reserved.
doi:10.1016/j.bbamem.2007.08.034

being reported [3–25]. In solution state NMR, some of these improvements include TROSY [26–29], clever isotopic labelling strategies [30–32], and the use of multiple detergents [33]. In solid state NMR, the use of bicelles [3,7,34–36], high-speed MAS [15,37], and/or novel pulse sequences (e.g. in [38–43]) has resulted in an explosion in the number of biomolecular studies, as compared to just a decade ago. In fact, the number of unique NMR structures of membrane peptides and proteins in the Protein Databank is about 10% of all known membrane protein structures reported to date. Most strikingly, all of these structures have been solved in the last 10 years. Despite these tremendous advances, many obstacles remain to be tackled.

One family of biomolecules that pose significant challenges to study by either solution and/or solid state NMR are the naturally occurring lipopeptides. Lipopeptides consist of linear or cyclic peptide sequences, with either net positive or negative charges, to which a fatty acid moiety is covalently attached at the N-terminus. They are a class of antibiotics that are highly active against multi-resistant bacteria. A number of lipopeptides consist of cationic amphiphilic peptides with an acetylated N-terminus (C8–C18 fatty acid chain length) [44–49]. Examples include members of the polymyxin family, which have been extensively studied [50–54]. In the anionic lipopeptide class, the first naturally occurring member to be discovered more than 50 years ago was amphomycin [55]. Additional members of this class of compounds include crystallomycin [56,57], aspartocin [58–61], glumamycin [62–64], laspartomycin [65], tsushimycin [66,67], and, by far the most-studied, daptomycin [68–73]. Because of their unique composition, they function in a manner that is atypical for most antibacterial agents, making them a unique class of antibiotics.

There are two major challenges in studying lipopeptides such as daptomycin, which is the focus of this contribution, by NMR. First, obtaining selective or uniformly isotopically labelled (^{13}C, ^{15}N, and/or ^{2}H) samples is difficult. Since daptomycin is a cyclic anionic tridecapeptide, with a number of D-amino acids (D-asparagine, D-alanine, and D-serine), 3 uncommon amino acid residues (ornithine, (2S,3R)-3-methyl-glutamic acid and kynurenine), and a N-terminus that is acylated with a n-decanoyl fatty acid side chain, biosynthesis or peptide synthesis by traditional routes is impossible. Although recent studies have demonstrated how daptomycin and analogues can be made by modifying the nonribosomal peptide synthetase (NRPS) in the daptomycin biosynthetic pathway, using either different strains of *Streptomyces roseosporus* [74,75] or *Streptomyces coelicolor* [76,77], production of large quantities of daptomycin, labelled to the high level required for structural studies has not been reported to date. The second difficulty in undertaking a structural study of daptomycin is the requirement of high concentrations of calcium (i.e. >1000 times the daptomycin concentration), in the form of Ca^{2+}, for activity [78–80]. Oligomerization occurs under conditions where calcium is added in a 1:1 Ca^{2+}/daptomycin molar ratio. This has recently been confirmed using equilibrium sedimentation [81] and solution state NMR [2,81,82] experiments, where upon addition of one molar equivalent of Ca^{2+}, a micelle consisting of 14–16 daptomycin molecules was formed. The lines observed in solution state NMR spectra under these conditions are broad, making even such a small peptide difficult to work with.

In order to understand the importance of calcium for the activity of daptomycin and to determine how daptomycin interacts with bacterial membranes, structural studies are essential. In the following, we will first briefly discuss a recently proposed mechanism of action [73], based on data of the interaction of daptomycin with divalent cations [81] and model membranes [83] obtained in our laboratories or through collaboration. In subsequent sections, we will present recent solution state NMR data obtained for daptomycin in DHPC micelles, obtained under different buffer/Ca^{2+} conditions. The implications of our results for the later steps in the mechanism of action of daptomycin will be discussed.

2. Mode of action of daptomycin

A number of papers and reviews have presented different views on the mode of action of daptomycin (for recent work see [73,84–89]). Many of these studies have shown that daptomycin displays rapid bactericidal activity by interacting with the cytoplasmic membrane in a calcium-dependent manner and oligomerizing in the membrane. As a result of this interaction, an efflux of potassium from the bacterial cell occurs, which in turn is proposed to lead to cell death, as this loss of potassium leads to dysfunction of macromolecular synthesis [86].

In addition to recently showing that the titration of calcium into a daptomycin solution leads to linebroadening in the NMR spectra, when Ca^{2+} is added in a 1:1 Ca^{2+}/daptomycin molar ratio, and that a micelle is formed, we have also demonstrated that the formation of this aggregate is not accompanied by a change in the structure of daptomycin, as originally proposed [1]. Indeed, when the divalent cation magnesium is added to daptomycin, the NOESY spectra closely resemble the NOESY spectra obtained for apo-daptomycin. Furthermore, re-interpreting the appearance of new NOE cross-peaks in the NOESY spectra of daptomycin in the presence of 1 equivalent of Ca^{2+} as being due to intermolecular contacts in the daptomycin micelle resulted in new structures, which were also quite similar to the apo-form [81]. This suggests that the interaction of daptomycin with Ca^{2+} is weak and non-perturbing. Given these findings, we propose that the first step in the mechanism of action of daptomycin is the formation of a loose micelle, which serves to deliver daptomycin to the bacterial membrane [73] in a "detergent-like" form (Fig. 1). This form would have a large membrane-disruptive potential, thereby allowing daptomycin to insert into the membrane rapidly and effectively (Fig. 1c).

It is interesting to note that there are three proposed structures of apo daptomycin [1,2,82], which are considerably different. For example, the backbone Cα RMSD between the 1T5M consensus structure [1] and 1XT7 (3.2 Å) [82] and the Rotondi and Gierasch structures (>4 Å, for each of the six structures reported in [2]) are large. The differences are even larger if the lipid tail and side chains are taken into account. We suggest that this wide spread of proposed structures reflects the very high mobility of daptomycin in the apo form. This high flexibility has significant consequences for structure determination and refinement using NOE restraints

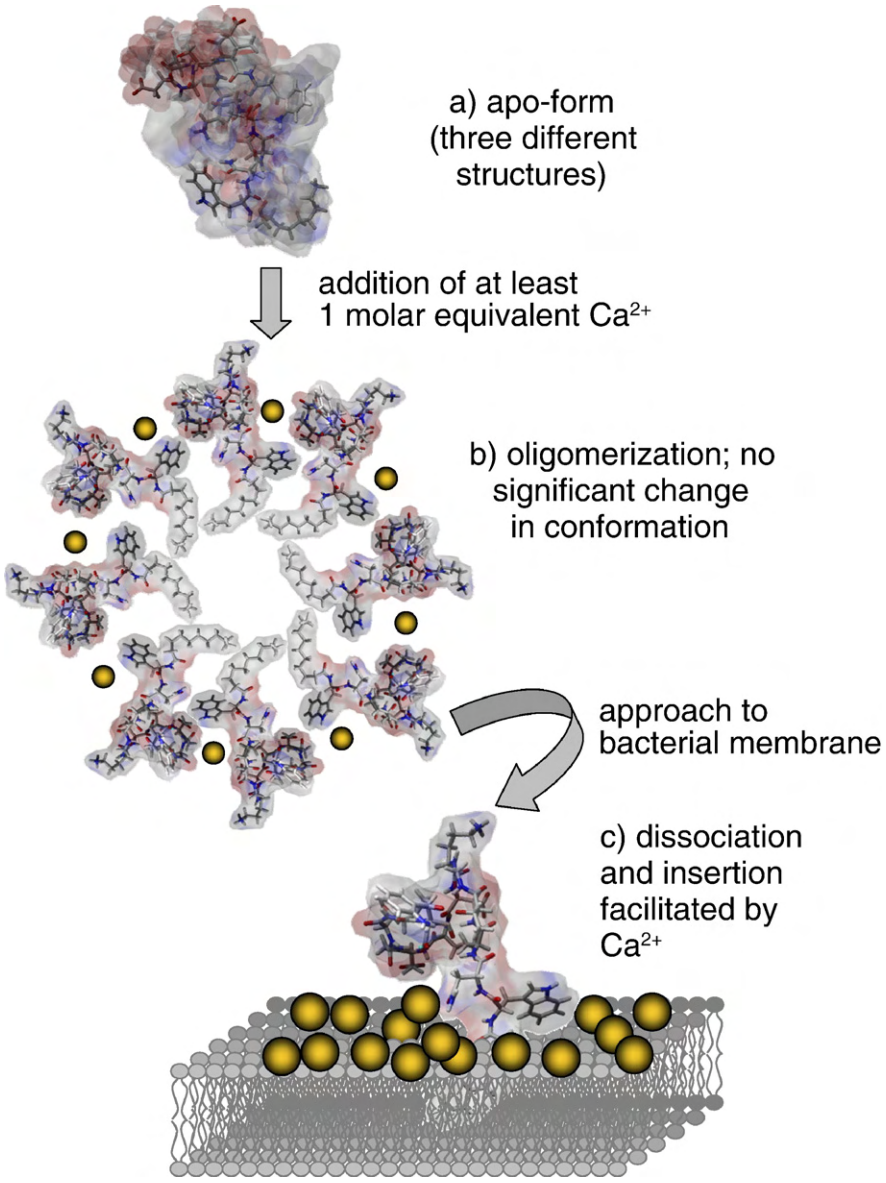

Fig. 1. Mechanism of action of daptomycin: (a) without calcium, daptomycin adopts a structure that is reasonably well defined but not highly amphiphilic. Three different structures have been reported in the literature [1,2,82]. Once a 1:1 calcium to daptomycin molar ratio is reached, the lipopeptide oligomerizes (b) to form a 14–16mer and most likely arranges itself into a micelle [81]. This process is not accompanied by a change in conformation, as originally proposed. (c) Once daptomycin comes into close proximity with the bacterial membrane, the multimer dissociates, and daptomycin inserts into the bilayer. Insertion of daptomycin into the membrane is accompanied by the induction of positive membrane curvature [83]. Oligomerization and/or conformational changes of daptomycin in the membrane may occur. Finally, bacterial cells are killed by membrane perforation (assessed as depolarization) or some other membrane-associated event (not shown).

because the number of observable long-range NOEs is thereby reduced. Indeed, the apo structures were each solved with relatively few inter-residue constraints (e.g. 29 for [2] and 35 for [1]), as compared to other membrane-associated peptides of a similar size (e.g. the structure of PW2 in SDS, a 12 residue peptide, was solved using 50 inter-residue constraints [90]). This reduction in the number of observed NOE restraints can lead to the overall protein structure being under-determined. A consequence of this is that, while it is possible to satisfy the observed experimental NOE restraints with a small set of protein structures, any such set cannot be truly representative of the sampled phase space in solution. This phenomenon has been noted before in connection with small mobile peptides [91].

The next steps in the mechanism involve the perturbation by daptomycin of bacterial membranes, and are mediated by a high concentration of calcium ions, which are known to interact more strongly with negatively charged lipid headgroups than do, say magnesium ions [92]. DSC and solid state ^{31}P NMR studies of daptomycin in the presence of 1-palmitoyl-2-oleoyl-*sn*-glycero-3-phosphocholine and 1-palmitoyl-2-oleoyl-*sn*-glycero-3-phospho-*rac*-1-glycerol (POPC/POPG) (1:1) lipid bilayers and Ca^{2+} have demonstrated the ability of daptomycin to perturb membranes [83] by inducing positive curvature strain on the lipids. Specifically, the data clearly indicates that the addition of daptomycin had a strong effect on the structural organization of acidic membranes in a manner dependent on Ca^{2+}. The addition

of 5 mM Ca^{2+} to pure DMPG bilayers resulted in a bilayer to hexagonal phase transition temperature of ≥62 °C, and caused only a minimal increase in vesicle size of large unilamellar POPC/POPG liposomes. On the other hand, the addition of daptomycin in the presence of 5 mM Ca^{2+} to DMPG resulted in the presence of an isotropic peak in the ^{31}P NMR spectra at temperatures of 21–80 °C, and a six-fold, non-uniform, increase in vesicle size of POPC/POPG liposomes. At this stage of the mechanism, daptomycin may also oligomerize in the membrane, but no evidence yet exists to support this proposal, which would be very difficult to characterize by analytical ultracentrifugation [93], for example. As a final step, leakage occurs and has been proposed to lead to cell death. It is also possible that daptomycin aggregation in the membrane would interfere with membrane-associated processes including synthesis of cell wall components, energetics, cell division etc.

To determine whether the interaction of daptomycin with lipids is accompanied by a change in structure, we undertook a solution state NMR study of daptomycin in DHPC micelles.

3. Daptomycin in micelles

Given the linebroadening observed in ^1H NMR spectra of 2 mM daptomycin prepared in a solution of 100 mM KCl, 0.2 mM EDTA, 5 mM $CaCl_2$, pH 6.70 [1], two sets of micelle samples were prepared. The first set was based on the conditions used by Rotondi and Gierasch, which yielded a "well defined" structure for the apo form [2]. Daptomycin was added in small portions to a sample buffer, consisting of 10 mM sodium phosphate, pH 5.3, 10% D_2O in H_2O (v/v), which was degassed using multiple cycles of the freeze–vacuum–thaw method. The final concentration of daptomycin was 1.9 mM in a 600 µl sample volume. ^1H NMR TOCSY [94] and NOESY [95] spectra of this sample were collected at 298 K and 313 K using a Bruker 500 MHz spectrometer, using a TXI SB 5-mm probe with *z* gradients, in phase-sensitive mode using time proportional phase incrementation (TPPI) [96] in the indirect dimension. The TOCSY experiment used the MLEV17 sequence for mixing (mixing time = 70 ms) and excitation sculpting with gradients for water suppression [97]. The 2D data set consisted of 4096 data points in t_2 and 256 points in t_1. The NOESY experiment was acquired with a mixing time of 150 ms and also used excitation sculpting for water suppression. The data size for this data set was the same as for the TOCSY spectrum. The spectra were referenced to the methyl resonance in 2,2-dimethyl-2-silapentane-5-sulfonate sodium salt (DSS) which resonates at 0 ppm and were processed to a final matrix dimension of 1024 × 1024 points, using a shifted sine bell weighting function in both dimensions. The spectra were analyzed using TOPSPIN from Bruker. The spectra yielded over one hundred well-defined NOE cross-peaks (Fig. 2a), similar to what was previously reported [2]. To this sample, fully deuterated 1,2-dihexanoyl-*sn*-glycero-3-phosphocholine (DHPC-d40) was added such that the daptomycin to lipid ratio was 1:50. TOCSY and NOESY spectra

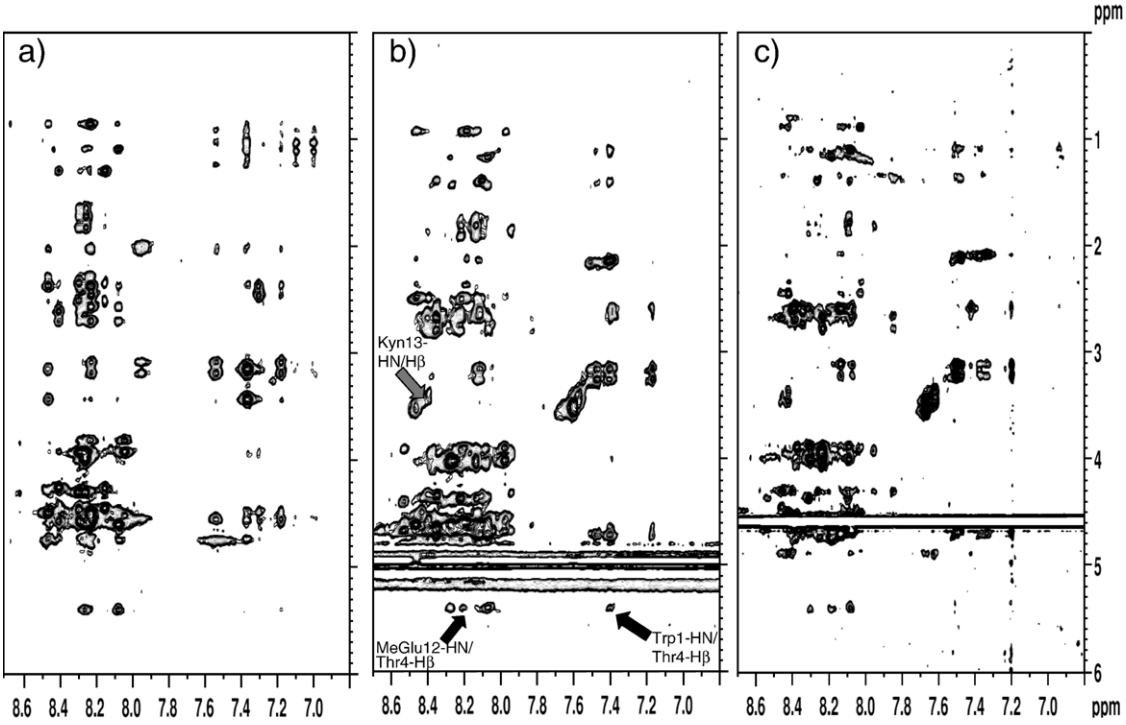

Fig. 2. Fingerprint region of solution NMR ^1H NOESY spectra of (a) daptomycin in phosphate buffer at 298 K, (b) daptomycin in DHPC and phosphate buffer at 313 K, and (c) daptomycin in DHPC micelles, 100 mM KCl, 0.2 mM EDTA, 5 mM $CaCl_2$, pH 6.70 at 318 K. For (a) and (b), the spectra were acquired using a phase sensitive NOESY experiment, with excitation sculpting with gradients for water suppression (see text). For (c), the spectra were acquired using WATERGATE [99] for water suppression (see text for further details). In all case, DHPC-d40 was added such that the daptomycin to DHPC ratio was 1:50 and the mixing time for the NOESY experiment was set to 150 ms. In panel b, black arrows indicate new NOE contacts which are not present in the NOESY spectrum of daptomycin in phosphate buffer alone. The grey arrow indicates the presence of multiple conformers (also found for the Trp1-Hε1/Trp1-Hδ1 NOE, for example—not shown). All spectra were referenced to external DSS (δ_{CH3} = 0 ppm).

were recorded using the same conditions as above, but at a temperature of 313 K. The spectra were referenced to external DSS. As before, 4k×256 points were acquired and the final processed spectrum consisted of a 1k×1k matrix in TOPSPIN. The resulting NOESY spectrum is shown in Fig. 2b. As indicated by the black and grey arrows, addition of DHPC led respectively to the presence of additional NOEs and to the presence of multiple conformers, as manifested by multiple resonances for the same spin system. For example, additional contacts between Trp1-HN/Thr4-Hβ and MeGlu12-HN/Thr4-Hβ (Fig. 2b) were found. Likewise, a number of contacts found in the micelle-free sample, such as NOEs between Asp7-HN/Ala8-Hβ or Gly10-HN/Asp9-Hβ1,2, were missing in the DHPC containing sample. A full summary of the long-range NOE contacts found in both samples is shown in Fig. 3. For both daptomycin in phosphate buffer and daptomycin in DHPC/phosphate buffer, a total of 34 long-range (i to i+1 or farther) contacts (some of which are to distinct Hα′s and Hβ′s) were found. As can be seen from the pattern of contacts which emerges in Fig. 3, the structure of daptomycin appeared to change upon interaction with micelles. A full structural calculation would be needed to determine the extent of this conformational change and is currently the subject of study in our laboratories.

The second sample that was prepared consisted of the buffer used by Jung et al. [1] to which DHPC-d40 was added, such that the daptomycin to DHPC ratio was 1:50, as before. The spectra were recorded on a Varian Unity500 spectrometer operated by the UBC Laboratory for Molecular Biophysics. Homonuclear TOCSY (spin lock time=60 ms) [94], NOESY (τ_m=150 ms) [95], and DQF-COSY [98] were collected at 318 K. WATERGATE [99] was used for water suppression in this case and the data matrices were 2k by 512. The spectra were referenced to external DSS and processed to yield a 2k×512 point matrix. The spectra were converted to Bruker format and analyzed using TOPSPIN. As in the case where the sample was prepared with DHPC/phosphate buffer, multiple conformers of daptomycin were observed, though in this case, there were many more additional peaks than under the phosphate/DHPC conditions (Fig. 2c). For example, multiple resonances were found for the Trp1-Hε1 crosspeak to Trp1-Hδ1, as well as for many resonances in Kyn13. A total of 150 NOE constraints were found, of which 63 were inter-residue contacts. It should be noted that the higher number of restraints found here is partly due to the fact that some H's give rise to multiple resonances. The NOE constraints were calibrated such that the NOE intensity for Trp1 Hδ1-Hε1 corresponds to 2.4 Å. Of the 150 experimental NOE constraints, only 114 could be unambiguously assigned to atom pairs and therefore be used in the subsequent refinement procedure. For example, all contacts to the n-decanoyl moiety were omitted, as it is impossible to unambiguously assign the ^{1}H resonances for the fatty acid chain in the spectra. Consequently, this part of the structure is completely undetermined by NMR in the structures reported here. Moreover, only one set of the contacts to side-chains which gave rise to multiple signals in the spectra (e.g. Trp1-Hε1 crosspeak to Trp1-Hδ1) was used. As is common practice, distance restraints to protons resulting from non-stereospecific resonance assignments were modelled using pseudo-atom locations [100].

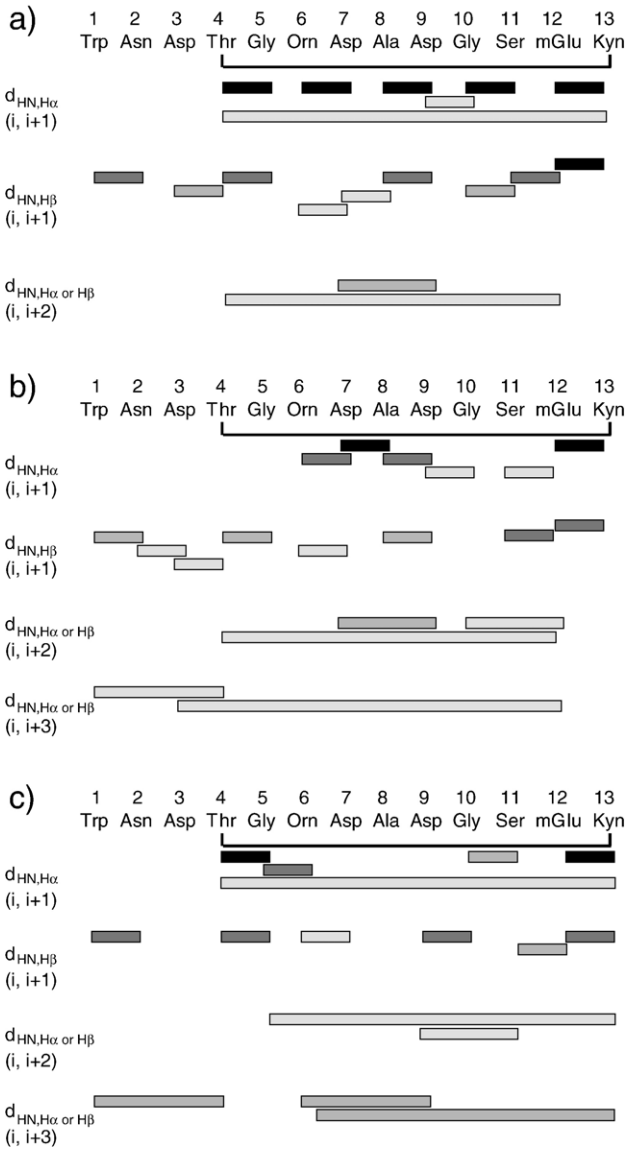

Fig. 3. Summary of the long-range NOE connectivities observed for (a) daptomycin in phosphate buffer at 298 K, (b) daptomycin in DHPC and phosphate buffer at 313 K, and (c) daptomycin in DHPC micelles, 100 mM KCl, 0.2 mM EDTA, 5 mM $CaCl_2$, pH 6.70 at 318 K. The progression from black to light grey bars indicates that the NOEs go from strong, to medium, to weak, to very weak, as per the standard definitions. The long bars are used because daptomycin is cyclic. Note that contacts between $d_{NN}(i, i+1)$ and $d_{NN}(i, i+2)$ are present for daptomycin under each condition, but due to overlap, these connectivities are not included in the comparison. For the sample in (a), $d_{NN}(i, i+1)$ contacts identified are between residues 1/2, 4/5, 6/7, 7/8, 8/9, and 12/13 and $d_{NN}(i, i+2)$ contacts identified are between residues 2/4 and 7/9. For the sample in (b), $d_{NN}(i, i+1)$ contacts identified are between residues 3/4, 8/9, and 12/13. For the sample in (c), $d_{NN}(i, i+1)$ contacts identified are between residues 4/5, 8/9, 11/12, and 12/13. Finally, for the sample in (c), many additional long range contacts (e.g. Asp7-HN to Kyn13-Hα) were found, but are not listed (see Table 1).

4. Daptomycin structure in DHPC in the presence of Ca^{2+}

Using the NOE restraints derived from the sample containing 2 mM daptomycin, DHPC, and buffer consisting of 100 mM

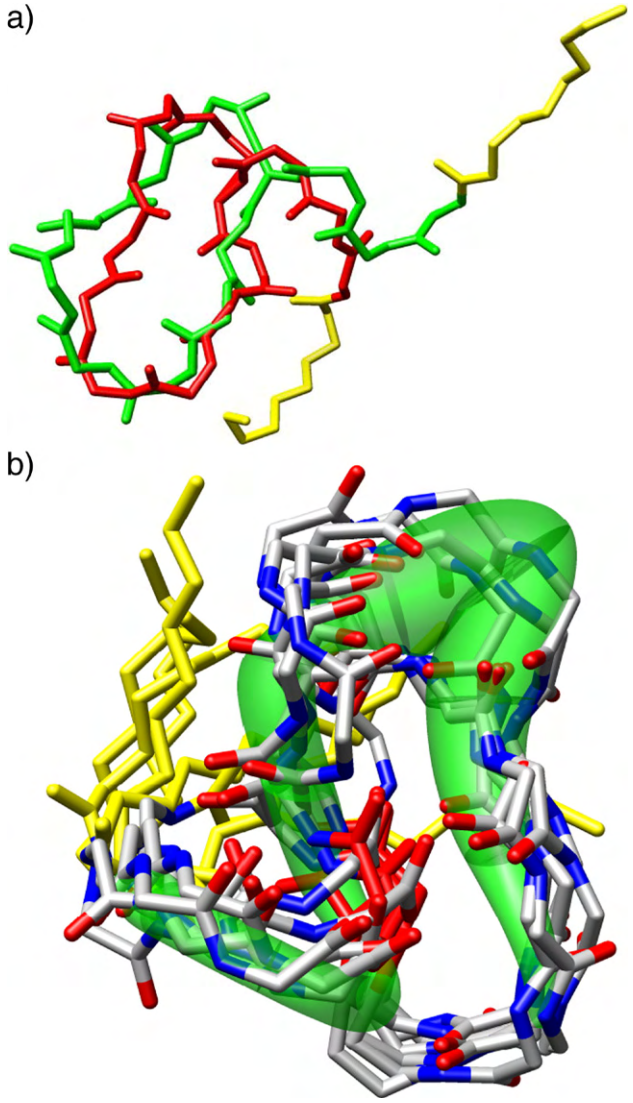

Fig. 4. Structure of daptomycin in DHPC micelles, 100 mM KCl, 0.2 mM EDTA, 5 mM $CaCl_2$, pH 6.70, derived from NOE data obtained at 318 K. (a) Predominant structure of daptomycin in DHPC micelles (red), compared to the consensus structure of apo-daptomycin, PDB entry 1T5 M (green). (b) 7 representative structures of daptomycin in DHPC micelles, shown as a backbone representation and as a worm (green), which was generated by taking the coordinates for each representative structure of clusters 0...6 and weighting them according to cluster size (see Section 4). In both (a) and (b) the fatty acid chain is represented in yellow.

KCl, 0.2 mM EDTA, 5 mM $CaCl_2$, pH 6.70, two sets of refinements were carried out. The protocol used was as previously described for the refinement of the calcium conjugated structure of daptomycin [81]. Briefly, refinement was performed using the GROMOS96 [100,101] biomolecular simulation package and the 43A1 force field [100]. The different models investigated were solvated in explicit SPC water [102]. Truncated octahedron periodic boundary conditions were imposed. Simulations were performed in the NPT ensemble (T= 300 K, P=1 atm) using the Berendsen weak coupling methods [103]. Covalent bonds were constrained using the SHAKE method [104], with a relative geometric tolerance of 10^{-4}. A reaction field [105] long-range correction to the truncated Coulomb potential was applied. For the first model, the 1T5M consensus structure was solvated with 1648 water molecules and energy minimised. A second model, starting from 1T5N, was also run but yielded poor structures so will not be discussed further. Initial velocities were generated from a Maxwell–Boltzmann distribution at 300 K after which the system was equilibrated for 1ns. At this point, the time-averaged distance restraining potential energy function [100,101,106] with a force constant of K_{dr}=2.49 kJ mol^{-1} nm^{-2} and relaxation time τ_{dr}= 20 ps, was switched on. This function is half-harmonic close to a NOE distance bound r_0 but reduces to a linear function at $r_0+\Delta r_h$ to avoid very high energies when distance restraints are severely violated. The value of Δr_h was set to 0.2 nm. The system was simulated for a further 10 ns for data collection. One thousand configurations, selected at 10 ps time intervals from this simulation, were subjected to a cluster analysis as previously described [81], where the clustering cut-off was set to 0.075 nm and all Cα atoms were considered in the distance metric. This resulted in a total of 26 clusters. In order to determine the dominant configurations in the ensemble of points, the largest n clusters were chosen such that the accumulated percentage is larger than 90% of the 1000 sampled points. This resulted in seven clusters, 0..6, in decreasing size (0: 43.2%, 1: 21.4%, 2: 10.0%, 3: 6.6%, 4: 3.7%, 5: 3.1%, 6: 3.0%). The representative structure from cluster 0 is shown in Fig. 4a, along with the apo form consensus 1T5M structure [1]. The seven representative structures of these clusters [81] (0…6) are shown in Fig. 4b and are deposited in the PDB file. The Cα RMSD between these structures and other statistics are reported in Tables 1–3. A comparison of this structure to other known daptomycin structures [1,2,81,82] is discussed in Section 6, after a brief examination of how daptomycin functions in the presence of PC membranes, with and without Ca^{2+}.

5. Biological relevance: daptomycin–PC interactions

As with all structural studies, a compromise must always be made between finding sample conditions that yield well-defined

Table 1
Statistical analysis for the NMR-derived structures of daptomycin in DHPC micelles, 100 mM KCl, 0.2 mM EDTA, 5 mM $CaCl_2$, pH 6.70

Number of NOE restraints	114
Number of intra-residue restraints	69
Number of inter-residue restraints	45
Total number of NOE restraints violated [a]	31
Total % of NOE violations [b]	27.2%
Total number of intra-residues restraints violated	14
Total number of inter-residues restraints violated	17
Average RMSD	
Cα—Residues 1–13	1.7±0.5 Å
Cα—Residues 4–13	1.5±0.4 Å
Average relative NOE violation calculated using the 1T5M restraints	0.014
Average relative NOE violation calculated using the 1T5N restraints	0.053

[a] A restraint is considered to be violated if the average relative violation is larger that 0.1. The average is over the entire 10 ns trajectory.
[b] Calculated from 31*100/114.

NMR spectra, and conditions that are biologically relevant. In the case of daptomycin, high Ca^{2+} concentrations and the presence of PC/PG lipids are needed for activity, conditions that are not amenable to solution state NMR studies, since in this case daptomycin causes fusion [83]. However, if studies are limited to PC lipids, as done here, it is possible to determine the structure of daptomycin in micelles, with and without calcium.

To quantify how daptomycin functions in the presence of PC lipids, with and without Ca^{2+}, we can examine previously reported results from lipid flip-flop and calcein release assays and fluorescence measurements [1]. Lipid flip-flop measures the movement of the fluorescently labelled lipid probe, C_6-NBD-PC, from the inner leaflet to the outer leaflet of the membrane bilayer and is considered one of the more sensitive methods for measuring peptide–lipid interactions. Normally, the movement of lipid molecules between the inner and outer leaflet is relatively slow; however, certain peptides like daptomycin in the presence of Ca^{2+}, magainin 2 [107], and various other cationic peptides [108] have been shown to greatly enhance the movement of lipids between the inner and outer leaflets. Daptomycin was able to induce between 25 and 45% lipid flip-flop in both PC/PG and PC liposomes with 2 mM Ca^{2+}. No lipid flip-flop was observed when daptomycin or Ca^{2+} was added separately to the labelled liposomes. The disruption and leakage of membranes due to the addition of daptomycin can be assessed by the release of calcein from either calcein-entrapped unilamellar PC or PC/PG liposomes. Calcein is a fluorescent dye that self-quenches its own fluorescence at the higher concentrations present within liposomes, and de-quenches upon its release. In our previous study [1], we found that pre-incubation of daptomycin with calcium was required for daptomycin to induce 80–100% leakage from calcein-loaded PC/PG liposomes. Although calcein leakage was much less efficient in PC liposomes (ca. 10%), it did occur, but again only in the presence of 2 or 5 mM Ca^{2+}. Finally, given that daptomycin contains two aromatic residues (Trp-1 and Kyn-13) that are intrinsically fluorescent, it is possible to monitor the insertion of these lipophilic residues into the phospholipid membrane environment. It was reported in [1], that in aqueous solution, daptomycin in both the presence and absence of Ca^{2+} was weakly fluorescent with an approximate maximum emission wavelength of 465 nm. Addition of neutral PC or acidic PC/PG (1:1) liposomes in the presence of Ca^{2+} was necessary to induce a blue shift and an increase in fluorescence intensity.

Table 2
Average relative NOE violations for each of the seven NMR-derived structures of daptomycin (clusters 0 to 6—see text) in DHPC micelles, 100 mM KCl, 0.2 mM EDTA, 5 mM $CaCl_2$, pH 6.70 calculated relative to the NOE restraints used in the structure calculation

Cluster number	Average relative NOE violations
0	0.162
1	0.156
2	0.170
3	0.155
4	0.177
5	0.168
6	0.177

Table 3
Comparison of how different each of the seven NMR-derived structures of daptomycin (clusters 0 to 6—see text) in DHPC micelles, 100 mM KCl, 0.2 mM EDTA, 5 mM $CaCl_2$, pH 6.70 is relative to known daptomycin structures (calculated as backbone Cα RMSDs): 1T5M.1 (consensus apo-daptomycin structure as reported in [1]), 1T5N.1 (consensus Ca^{2+}-conjugated structure from [1]), 1XT7 (apo-daptomycin structure as reported in [82]), and finally the apo-daptomycin structures reported in [2] (6 structures are reported, so we list the best (min), worst (max), and average (ave) fit between our structures and theirs)

Representative structure from cluster number	1T5M.1	1T5N.1	1XT7	Rotondi and Gierasch		
				Min	Max	Ave
0	3.0	4.5	3.2	4.1	4.7	4.4
1	3.7	4.9	3.1	4.6	5.3	4.9
2	3.5	4.5	3.1	4.2	4.9	4.6
3	3.1	4.3	3.4	4.0	4.7	4.4
4	3.3	4.9	2.7	4.6	5.1	4.9
5	2.9	4.8	3.2	4.5	5.1	4.8
6	2.8	4.0	3.6	3.8	4.4	4.1

Taken together, these data show that it is critical to study the structure of daptomycin in the presence of Ca^{2+} while DHPC provides a reasonable surrogate for membrane bilayers that are critical determinants of daptomycin action, despite the added complication of having to deal with multiple conformers as discussed above.

6. Conclusions and perspective

The resulting structure of daptomycin in DHPC micelles, in the presence of Ca^{2+}, is an extended ring, much like apo daptomycin (Fig. 4a). The backbone Cα RMSDs between the representative structure of the largest cluster (cluster 0), i.e. the one which is most sampled during the MD simulation, and each of the three apo structures are: 3.0 Å for the 1T5M consensus structure [1], 3.2 Å for 1XT7 [82], and between 4.1 and 4.7 Å for the Rotondi and Gierasch structures [2]. The backbone Cα RMSD between this same cluster 0 structure and the calcium-conjugated form recently described in [81] is 3.9 Å. In contrast, the backbone Cα RMSD between the daptomycin/DHPC structure and the calcium-bound form 1T5N is much larger, with a value of 4.5 Å. As can be seen from Tables 2 and 3, the other representative structures sampled (cluster 1…6) and illustrated in Fig. 4b have similar average relative NOE violations to the one obtained for cluster 0. Moreover, a comparison between the backbone RMSDs for each representative structure and other known daptomycin structures, namely 1T5M.1 (consensus apo-daptomycin structure as reported in [1]), 1T5N.1 (consensus Ca^{2+}-conjugated structure from [1]), 1XT7 (apo-daptomycin structure as reported in [82]), and the apo-daptomycin structures reported in [2], shows that there is no similarity between the representative structures for each cluster and other published structures. Since the RMSDs are smallest when calculated relative to 1T5M and 1XT7 (Table 3) and since the violations calculated relative to the apo form dataset are lowest (Table 1), this suggests that daptomycin undergoes only a minor conformational rearrangement upon binding with DHPC in the presence

of Ca^{2+}. This would indicate that the mechanism proposed in Fig. 1 is not accompanied by well defined, large structural rearrangements. Rather, daptomycin has a high degree of plasticity, allowing it to readily adapt to one environment, namely forming a micelle with Ca^{2+} at the intermolecular interfaces, or another, i.e. daptomycin embedded in lipids with Ca^{2+} at the daptomycin/lipid interface.

Much remains to be understood about how the rapid bactericidal activity of daptomycin is related to its dynamic nature and its interaction with the cytoplasmic membrane and whether oligomerization in the membrane is crucial. NMR may be able to provide some further insights in this regard. For example, H/D exchange and relaxation experiments would provide insight on the dynamics of daptomycin. Furthermore, solid state NMR methods could be used to determine the conformation of daptomycin in PC/PG membranes, as is commonly done for fusion peptides [109–119]. Furthermore, solid state NMR may be used to characterize the oligomerization state of daptomycin in PC and PC/PG bilayers [120,121]. The advent of new biosynthetic strategies [74–77] for the production of daptomycin will make such studies possible and further our understanding of how lipopeptides function.

Acknowledgements

The authors would like to thank the many co-workers who were involved in different aspects of the work on daptomycin: Jon-Paul Powers, Mark Okon, Steven W. Ho, Annett Rozek, Jennifer Calhoun, James D. Lear, John T.J. Cheng, and Jared Silverman. SKS gratefully acknowledges the support of NSERC through a Discovery Grant and a University Faculty Award and UBC. REWH was funded by CIHR and is the recipient of a Canada Research Chair. This project was also funded in part by Cubist Pharmaceuticals through grants to REWH and to SKS.

The coordinates of the micelle-bound structure of daptomycin in the presence of Ca^{2+} will be deposited in the Protein Databank and the BioMagResBank, and released upon publication.

Appendix A. Supplementary data

Supplementary data associated with this article can be found, in the online version, at doi:10.1016/j.bbamem.2007.08.034.

References

[1] D. Jung, A. Rozek, M. Okon, R.E.W. Hancock, Structural transitions as determinants of the action of the calcium-dependent antibiotic daptomycin, Chem. Biol. 11 (2004) 949–957.
[2] K.S. Rotondi, L.M. Gierasch, A well-defined amphipathic conformation for the calcium-free cyclic lipopeptide antibiotic, daptomycin, in aqueous solution, Biopolymers 80 (2005) 374–385.
[3] A.A. De Angelis, S.C. Howell, A.A. Nevzorov, S.J. Opella, Structure determination of a membrane protein with two trans-membrane helices in aligned phospholipid bicelles by solid-state NMR spectroscopy, J. Am. Chem. Soc. 128 (2006) 12256–12267.
[4] S.C. Howell, M.F. Mesleh, S.J. Opella, NMR structure determination of a membrane protein with two transmembrane helices in micelles: MerF of the bacterial mercury detoxification system, Biochemistry 44 (2005) 5196–5206.
[5] R.C. Page, J.D. Moore, H.B. Nguyen, M. Sharma, R. Chase, F.P. Gao, C.K. Mobley, C.R. Sanders, L. Ma, F.D. Sonnichsen, S. Lee, S. C. Howell, S.J. Opella, T.A. Cross, Comprehensive evaluation of solution nuclear magnetic resonance spectroscopy sample preparation for helical integral membrane proteins, J. Struct. Funct. Genomics 7 (2006) 51–64.
[6] S.H. Park, A.A. De Angelis, A.A. Nevzorov, C.H. Wu, S.J. Opella, Three-dimensional structure of the transmembrane domain of Vpu from HIV-1 in aligned phospholipid bicelles, Biophys. J. 91 (2006) 3032–3042.
[7] S.H. Park, S. Prytulla, A.A. De Angelis, J.M. Brown, H. Kiefer, S.J. Opella, High-resolution NMR spectroscopy of a GPCR in aligned bicelles, J. Am. Chem. Soc. 128 (2006) 7402–7403.
[8] C.M. Franzin, X.M. Gong, K. Thai, J. Yu, F.M. Marassi, NMR of membrane proteins in micelles and bilayers: the FXYD family proteins, Methods 41 (2007) 398–408.
[9] P. Teriete, C.M. Franzin, J. Choi, F.M. Marassi, Structure of the Na, K-ATPase regulatory protein FXYD1 in micelles, Biochemistry 46 (2007) 6774–6783.
[10] J. Hu, T. Asbury, S. Achuthan, C. Li, R. Bertram, J.R. Quine, R. Fu, T.A. Cross, Backbone structure of the amantadine-blocked trans-membrane domain m2 proton channel from influenza a virus, Biophys. J. 92 (2007) 4335–4343.
[11] C. Li, P. Gao, H. Qin, R. Chase, P.L. Gor'kov, W.W. Brey, T.A. Cross, Uniformly aligned full-length membrane proteins in liquid crystalline bilayers for structural characterization, J. Am. Chem. Soc. 129 (2007) 5304–5305.
[12] C.R. Sanders, F. Sonnichsen, Solution NMR of membrane proteins: practice and challenges, Magn. Reson. Chem. 44 (2006) S24–S40 (Spec No).
[13] J.H. Chill, J.M. Louis, J.L. Baber, A. Bax, Measurement of 15N relaxation in the detergent-solubilized tetrameric KcsA potassium channel, J. Biomol. NMR 36 (2006) 123–136.
[14] P.M. Hwang, W.Y. Choy, E.I. Lo, L. Chen, J.D. Forman-Kay, C.R. Raetz, G.G. Prive, R.E. Bishop, L.E. Kay, Solution structure and dynamics of the outer membrane enzyme PagP by NMR, Proc. Natl. Acad. Sci. U. S. A. 99 (2002) 13560–13565.
[15] O.C. Andronesi, J.R. Pfeifer, L. Al-Momani, S. Ozdirekcan, D.T. Rijkers, B. Angerstein, S. Luca, U. Koert, J.A. Killian, M. Baldus, Probing membrane protein orientation and structure using fast magic-angle-spinning solid-state NMR, J. Biomol. NMR 30 (2004) 253–265.
[16] M. Etzkorn, S. Martell, O.C. Andronesi, K. Seidel, M. Engelhard, M. Baldus, Secondary structure, dynamics, and topology of a seven-helix receptor in native membranes, studied by solid-state NMR spectroscopy, Angew. Chem., Int. Ed. Engl. 46 (2007) 459–462.
[17] A. Lange, K. Giller, O. Pongs, S. Becker, M. Baldus, Two-dimensional solid-state NMR applied to a chimeric potassium channel, J. Recept. Signal Transduct. Res. 26 (2006) 379–393.
[18] C. Fernandez, C. Hilty, S. Bonjour, K. Adeishvili, K. Pervushin, K. Wuthrich, Solution NMR studies of the integral membrane proteins OmpX and OmpA from *Escherichia coli*, FEBS Lett. 504 (2001) 173–178.
[19] A. Arora, F. Abildgaard, J.H. Bushweller, L.K. Tamm, Structure of outer membrane protein A transmembrane domain by NMR spectroscopy, Nat. Struct. Biol. 8 (2001) 334–338.
[20] T.P. Roosild, J. Greenwald, M. Vega, S. Castronovo, R. Riek, S. Choe, NMR structure of Mistic, a membrane-integrating protein for membrane protein expression, Science 307 (2005) 1317–1321.
[21] K. Oxenoid, J.J. Chou, The structure of phospholamban pentamer reveals a channel-like architecture in membranes, Proc. Natl. Acad. Sci. U. S. A. 102 (2005) 10870–10875.
[22] J.J. Buffy, B.A. Buck-Koehntop, F. Porcelli, N.J. Traaseth, D.D. Thomas, G. Veglia, Defining the intramembrane binding mechanism of sarcolipin to calcium ATPase using solution NMR spectroscopy, J. Mol. Biol. 358 (2006) 420–429.
[23] N.J. Traaseth, J.J. Buffy, J. Zamoon, G. Veglia, Structural dynamics and topology of phospholamban in oriented lipid bilayers using multidimensional solid-state NMR, Biochemistry 45 (2006) 13827–13834.
[24] F. Porcelli, B. Buck, D.K. Lee, K.J. Hallock, A. Ramamoorthy, G. Veglia, Structure and orientation of pardaxin determined by NMR experiments in model membranes, J. Biol. Chem. 279 (2004) 45815–45823.

[25] F. Porcelli, B.A. Buck-Koehntop, S. Thennarasu, A. Ramamoorthy, G. Veglia, Structures of the dimeric and monomeric variants of magainin antimicrobial peptides (MSI-78 and MSI-594) in micelles and bilayers, determined by NMR spectroscopy, Biochemistry 45 (2006) 5793–5799.
[26] K. Pervushin, R. Riek, G. Wider, K. Wuthrich, Attenuated T2 relaxation by mutual cancellation of dipole–dipole coupling and chemical shift anisotropy indicates an avenue to NMR structures of very large biological macromolecules in solution, Proc. Natl. Acad. Sci. U. S. A. 94 (1997) 12366–12371.
[27] R. Riek, K. Pervushin, K. Wuthrich, TROSY and CRINEPT: NMR with large molecular and supramolecular structures in solution, Trends Biochem. Sci. 25 (2000) 462–468.
[28] C. Tian, M.D. Karra, C.D. Ellis, J. Jacob, K. Oxenoid, F. Sonnichsen, C.R. Sanders, Membrane protein preparation for TROSY NMR screening, Methods Enzymol. 394 (2005) 321–334.
[29] V. Tugarinov, R. Sprangers, L.E. Kay, Line narrowing in methyl-TROSY using zero-quantum 1H-13C NMR spectroscopy, J. Am. Chem. Soc. 126 (2004) 4921–4925.
[30] K.H. Gardner, M.K. Rosen, L.E. Kay, Global folds of highly deuterated, methyl-protonated proteins by multidimensional NMR, Biochemistry 36 (1997) 1389–1401.
[31] V. Tugarinov, V. Kanelis, L.E. Kay, Isotope labeling strategies for the study of high-molecular-weight proteins by solution NMR spectroscopy, Nat. Protoc. 1 (2006) 749–754.
[32] N.K. Goto, K.H. Gardner, G.A. Mueller, R.C. Willis, L.E. Kay, A robust and cost-effective method for the production of Val, Leu, Ile (delta 1) methyl-protonated 15N-, 13C-, 2H-labeled proteins, J. Biomol. NMR 13 (1999) 369–374.
[33] C.P. Jaroniec, J.D. Kaufman, S.J. Stahl, M. Viard, R. Blumenthal, P.T. Wingfield, A. Bax, Structure and dynamics of micelle-associated human immunodeficiency virus gp41 fusion domain, Biochemistry 44 (2005) 16167–16180.
[34] U.H. Durr, K. Yamamoto, S.C. Im, L. Waskell, A. Ramamoorthy, Solid-state NMR reveals structural and dynamical properties of a membrane-anchored electron-carrier protein, cytochrome b5, J. Am. Chem. Soc. 129 (2007) 6670–6671.
[35] S.V. Dvinskikh, U.H. Durr, K. Yamamoto, A. Ramamoorthy, High-resolution 2D NMR spectroscopy of bicelles to measure the membrane interaction of ligands, J. Am. Chem. Soc. 129 (2007) 794–802.
[36] S.V. Dvinskikh, K. Yamamoto, U.H. Durr, A. Ramamoorthy, Sensitivity and resolution enhancement in solid-state NMR spectroscopy of bicelles, J. Magn. Reson. 184 (2007) 228–235.
[37] A. Samoson, T. Tuherm, Z. Gan, High-field high-speed MAS resolution enhancement in 1 H NMR spectroscopy of solids, Solid State Nucl. Magn. Reson. 20 (2001) 130–136.
[38] G. De Paepe, M.J. Bayro, J. Lewandowski, R.G. Griffin, Broadband homonuclear correlation spectroscopy at high magnetic fields and MAS frequencies, J. Am. Chem. Soc. 128 (2006) 1776–1777.
[39] M. Veshtort, R.G. Griffin, High-performance selective excitation pulses for solid- and liquid-state NMR spectroscopy, ChemPhysChem 5 (2004) 834–850.
[40] M. Baldus, Molecular interactions investigated by multi-dimensional solid-state NMR, Curr. Opin. Struct. Biol. 16 (2006) 618–623.
[41] C.H. Wu, A. Ramamoorthy, S.J. Opella, High-resolution heteronuclear dipolar solid-state NMR-spectroscopy, J. Magn. Reson., Ser. A 109 (1994) 270–272.
[42] A. Ramamoorthy, C.H. Wu, S.J. Opella, Experimental aspects of multidimensional solid-state NMR correlation spectroscopy, J. Magn. Reson. 140 (1999) 131–140.
[43] A. Ramamoorthy, Y.F. Wei, D.K. Lee, PISEMA solid-state NMR spectroscopy, Advances in solid state NMR studies of materials and polymers: a special volume dedicated to Isao Ando, vol. 52, 2004, pp. 1–52.
[44] A.F. Chu-Kung, K.N. Bozzelli, N.A. Lockwood, J.R. Haseman, K.H. Mayo, M.V. Tirrell, Promotion of peptide antimicrobial activity by fatty acid conjugation, Bioconjug. Chem. 15 (2004) 530–535.
[45] N.A. Lockwood, J.R. Haseman, M.V. Tirrell, K.H. Mayo, Acylation of SC4 dodecapeptide increases bactericidal potency against gram-positive bacteria, including drug-resistant strains, Biochem. J. 378 (2004) 93–103.
[46] H. Wakabayashi, H. Matsumoto, K. Hashimoto, S. Teraguchi, M. Takase, H. Hayasawa, N-acylated and D enantiomer derivatives of a nonamer core peptide of lactoferricin B showing improved antimicrobial activity, Antimicrob. Agents Chemother. 43 (1999) 1267–1269.
[47] P. Mak, J. Pohl, A. Dubin, M.S. Reed, S.E. Bowers, M.T. Fallon, W.M. Shafer, The increased bactericidal activity of a fatty acid-modified synthetic antimicrobial peptide of human cathepsin G correlates with its enhanced capacity to interact with model membranes, Int. J. Antimicrob. Agents 21 (2003) 13–19.
[48] R.M. Epand, Biophysical studies of lipopeptide–membrane interactions, Biopolymers 43 (1997) 15–24.
[49] S. Thennarasu, D.K. Lee, A. Tan, U. Prasad Kari, A. Ramamoorthy, Antimicrobial activity and membrane selective interactions of a synthetic lipopeptide MSI-843, Biochim. Biophys. Acta 1711 (2005) 49–58.
[50] L. Zhang, P. Dhillon, H. Yan, S. Farmer, R.E.W. Hancock, Interactions of bacterial cationic peptide antibiotics with outer and cytoplasmic membranes of *Pseudomonas aeruginosa*, Antimicrob. Agents Chemother. 44 (2000) 3317–3321.
[51] R.E.W. Hancock, D.S. Chapple, Peptide antibiotics, Antimicrob. Agents Chemother. 43 (1999) 1317–1323.
[52] D.R. Storm, K.S. Rosenthal, P.E. Swanson, Polymyxin and related peptide antibiotics, Ann. Rev. Biochem. 46 (1977) 723–763.
[53] I.R. Miller, D. Bach, M. Teuber, Effect of polymyxin B on the structure and the stability of lipid layers, J. Membr. Biol. 39 (1978) 49–56.
[54] M. Teuber, J. Bader, Action of polymyxin B on bacterial membranes: phosphatidylglycerol- and cardiolipin-induced susceptibility to polymyxin B in *Acholeplasma laidlawii* B, Antimicrob. Agents Chemother. 9 (1976) 26–35.
[55] B. Heinemann, M.A. Kaplan, R.D. Muir, I.R. Hooper, Amphomycin, a new antibiotic, Antibiot. Chemother. 3 (1953) 1239–1242.
[56] N.N. Lomakina, M.G. Brazhnikova, Chemical composition of crystallomycin, Biokhimiia 24 (1959) 425–431.
[57] L.E. Gol'Dberg, Pharmacological investigations on the antibiotic crystallomycin, Antibiotiki 4 (1959) 63–67.
[58] M.A. Darken, A.L. Jensen, P. Shu, Aspartocin. II. Fermentation studies, Antibiot. Annu. 7 (1959) 199–204.
[59] E.J. Kirsch, A.C. Dornbush, E.J. Backus, Aspartocin. III. In vitro antimicrobial properties, Antibiot. Annu. 7 (1959) 205–212.
[60] G.S. Redin, C.M. Mc, Aspartocin. IV. Activity against experimental infections in mice, Antibiot. Annu. 7 (1959) 213–219.
[61] A.J. Shay, J. Adam, J.H. Martin, W.K. Hausmann, P. Shu, N. Bohonos, Aspartocin. I. Production, isolation, and characteristics, Antibiot. Annu. 7 (1959) 194–198.
[62] M. Fujino, On glumamycin, a new antibiotic. VI. An approach to the amino acid sequence, Bull. Chem. Soc. Jpn. 38 (1965) 517–522.
[63] M. Fujino, M. Inoue, J. Ueyanagi, A. Miyake, On glumamycin, a new antibiotic. V. The steric configuration of alpha, beta-diaminobutyric acid, Bull. Chem. Soc. Jpn. 38 (1965) 515–517.
[64] M. Shibata, T. Kanzaki, K. Nakazawa, M. Inoue, H. Hitomi, K. Mizuno, M. Fujino, M. Akira, On glumamycin, a new antibiotic, J. Antibiot. (Tokyo) 15 (1962) 1–6.
[65] H. Naganawa, M. Hamada, K. Maeda, Y. Okami, T. Takeushi, Laspartomycin, a new anti-staphylococcal peptide, J. Antibiot. (Tokyo) 21 (1968) 55–62.
[66] J. Shoji, H. Otsuka, Studies on tsushimycin. II. The structures of constituent fatty acids, J. Antibiot. (Tokyo) 22 (1969) 473–479.
[67] J.I. Shoji, S. Kozuki, S. Okamoto, R. Sakazaki, H. Otsuka, Studies on tsushimycin. I. Isolation and characterization of an acidic acylpeptide containing a new fatty acid, J. Antibiot. (Tokyo) 21 (1968) 439–443.
[68] R.L. Hodinka, K. Jack-Wait, N. Wannamaker, T.P. Walden, P.H. Gilligan, Comparative in vitro activity of LY146032 (daptomycin), a new lipopeptide antimicrobial, Eur. J. Clin. Microbiol. 6 (1987) 100–103.
[69] N.E. Allen, J.N. Hobbs, W.E. Alborn Jr., Inhibition of peptidoglycan biosynthesis in gram-positive bacteria by LY146032, Antimicrob. Agents Chemother. 31 (1987) 1093–1099.
[70] A.S. Bayer, J. Yih, L. Hirano, LY146032 compared with penicillin G in experimental aortic valve endocarditis caused by group G streptococci, Antimicrob. Agents Chemother. 32 (1988) 141–143.

[71] P.L. Botha, C.J. van Heerden, E. Vorster, E.C. Venter, In vitro evaluation of the cyclic lipopeptide LY 146032 (daptomycin), S. Afr. Med. J. 74 (1988) 16–18.
[72] F. Ehlert, H.C. Neu, In vitro activity of LY146032 (daptomycin), a new peptolide, Eur. J. Clin. Microbiol. 6 (1987) 84–90.
[73] S.K. Straus, R.E. Hancock, Mode of action of the new antibiotic for Gram-positive pathogens daptomycin: comparison with cationic antimicrobial peptides and lipopeptides, Biochim. Biophys. Acta 1758 (2006) 1215–1223.
[74] R.H. Baltz, P. Brian, V. Miao, S.K. Wrigley, Combinatorial biosynthesis of lipopeptide antibiotics in *Streptomyces roseosporus*, J. Ind. Microbiol. Biotech. (2005) 1–9.
[75] K.T. Nguyen, D. Ritz, J.Q. Gu, D. Alexander, M. Chu, V. Miao, P. Brian, R.H. Baltz, Combinatorial biosynthesis of novel antibiotics related to daptomycin, Proc. Natl. Acad. Sci. U. S. A. 103 (2006) 17462–17467.
[76] J. Grunewald, S.A. Sieber, C. Mahlert, U. Linne, M.A. Marahiel, Synthesis and derivatization of daptomycin: a chemoenzymatic route to acidic lipopeptide antibiotics, J. Am. Chem. Soc. 126 (2004) 17025–17031.
[77] F. Kopp, J. Grunewald, C. Mahlert, M.A. Marahiel, Chemoenzymatic design of acidic lipopeptide hybrids: new insights into the structure–activity relationship of daptomycin and A54145, Biochemistry 45 (2006) 10474–10481.
[78] J.H. Andrew, M.C. Wale, L.J. Wale, D. Greenwood, The effect of cultural conditions on the activity of LY146032 against staphylococci and streptococci, J. Antimicrob. Chemother. 20 (1987) 213–221.
[79] A.W. Chow, N. Cheng, In vitro activities of daptomycin (LY146032) and paldimycin (U-70,138F) against anaerobic gram-positive bacteria, Antimicrob. Agents Chemother. 32 (1988) 788–790.
[80] G.M. Eliopoulos, S. Willey, E. Reiszner, P.G. Spitzer, G. Caputo, R.C. Moellering Jr., In vitro and in vivo activity of LY 146032, a new cyclic lipopeptide antibiotic, Antimicrob. Agents Chemother. 30 (1986) 532–535.
[81] S.W., Ho, D., Jung, J.R., Calhoun, J.D., Lear, M., Okon, W.R.P., Scott, R.E., Hancock and S.K., Straus, Eur. Biophys. J. in press.
[82] L.J. Ball, C.M. Goult, J.A. Donarski, J. Micklefield, V. Ramesh, NMR structure determination and calcium binding effects of lipopeptide antibiotic daptomycin, Org. Biomol. Chem. 2 (2004) 1872–1878.
[83] D., Jung, J.P., Powers, S.K., Straus, R.E., Hancock, Chem. Phys. Lipids. submitted for publication.
[84] D. Abbanat, M. Macielag, K. Bush, Novel antibacterial agents for the treatment of serious gram-positive infections, Expert Opin. Investig. Drugs 12 (2003) 379–399.
[85] J.D. Alder, Daptomycin: a new drug class for the treatment of gram-positive infections, Drugs Today (Barc.) 41 (2005) 81–90.
[86] J.A. Silverman, N.G. Perlmutter, H.M. Shapiro, Correlation of daptomycin bactericidal activity and membrane depolarization in *Staphylococcus aureus*, Antimicrob. Agents Chemother. 47 (2003) 2538–2544.
[87] R.E.W. Hancock, Mechanisms of action of newer antibiotics for gram-positive pathogens, Lancet, Infect. Dis. 5 (2005) 209–218.
[88] J.N. Steenbergen, J. Alder, G.M. Thorne, F.P. Tally, Daptomycin: a lipopeptide antibiotic for the treatment of serious gram-positive infections, J. Antimicrob. Chemother. 55 (2005) 283–288.
[89] P.M. Shah, The need for new therapeutic agents: what is the pipeline? Clin. Microbiol. Infect. 11 (Suppl 3) (2005) 36–42.
[90] L.W. Tinoco, A. Da Silva Jr., A. Leite, A.P. Valente, F.C. Almeida, NMR structure of PW2 bound to SDS micelles. A tryptophan-rich anticoccidial peptide selected from phage display libraries, J. Biol. Chem. 277 (2002) 36351–36356.
[91] X. Daura, I. Antes, W.F. van Gunsteren, W. Thiel, A.E. Mark, The effect of motional averaging on the calculation of NMR-derived structural properties, Proteins 36 (1999) 542–555.
[92] P. Garidel, A. Blume, 1,2-Dimyristoyl-sn-glycero-3-phosphoglycerol (DMPG) monolayers: influence of temperature, pH, ionic strength and binding of alkaline earth cations, Chem. Phys. Lipids 138 (2005) 50–59.
[93] D. Noy, J.R. Calhoun, J.D. Lear, Direct analysis of protein sedimentation equilibrium in detergent solutions without density matching, Anal. Biochem. 320 (2003) 185–192.
[94] L. Braunschweiler, R.R. Ernst, Coherence transfer by isotropic mixing: application to proton correlation spectroscopy, J. Magn. Reson. 53 (1983) 521–528.
[95] J. Jeener, B.H. Meier, P. Bachmann, R.R. Ernst, Investigation of exchange processes by two-dimensional NMR spectroscopy, J. Chem. Phys. 71 (1979) 4546–4553.
[96] D. Marion, K. Wuthrich, Application of phase sensitive two-dimensional correlated spectroscopy (COSY) for measurements of 1H–1H spin–spin coupling constants in proteins, Biochem. Biophys. Res. Commun. 113 (1983) 967–974.
[97] T.L. Hwang, A.J. Shaka, Water suppression that works—excitation sculpting using arbitrary wave-forms and pulsed-field gradients, J. Magn. Reson., Ser. A 112 (1995) 275–279.
[98] M. Rance, O. Sorensen, G. Bodenhausen, G. Wagner, R.R. Ernst, K. Wüthrich, Improved spectral resolution in cosy 1H NMR spectra of proteins via double quantum filtering, Biochem. Biophys. Res. Commun. 117 (1983) 479–485.
[99] M. Piotto, V. Saudek, V. Sklenar, Gradient-tailored excitation for single-quantum NMR spectroscopy of aqueous solutions, J. Biomol. NMR 2 (1992) 661–665.
[100] W.F. van Gunsteren, S.R. Billeter, A.A. Eising, P.H. Huenenberger, P. Krueger, A.E. Mark, W.R.P. Scott, I.G. Tironi, Biomolecular simulation: the GROMOS96 manual and user guide. VdF: Hochschulverlag AG an der ETH Zurich BIOMOS b.v., Zurich, Groningen, , 1996.
[101] W.R.P. Scott, P.H. Hunenberger, I.G. Tironi, A.E. Mark, S.R. Billeter, J. Fennen, A.E. Torda, T. Huber, P. Kruger, W.F. van Gunsteren, The GROMOS biomolecular simulation program package, J. Phys. Chem., A Mol. Spectrosc. Kinet. Environ. Gen. Theory 103 (1999) 3596–3607.
[102] H.J.C. Berendsen, J.P.M. Postma, W.F. van Gunsteren, J. Hermans, in: B. Pullman (Ed.), Intermolecular Forces, Reidel, Dordrecht, 1981, pp. 331–342.
[103] H.J.C. Berendsen, J.P.M. Postma, W.F. van Gunsteren, A. Dinola, J.R. Haak, Molecular-dynamics with coupling to an external bath, J. Chem. Phys. 81 (1984) 3684–3690.
[104] J.P. Ryckaert, G. Ciccotti, H.J.C. Berendsen, Numerical-Integration of cartesian equations of motion of a system with constraints — molecular-dynamics of n-alkanes, J. Comput. Phys. 23 (1977) 327–341.
[105] I.G. Tironi, R. Sperb, P.E. Smith, W.F. van Gunsteren, A generalized reaction field method for molecular-dynamics simulations, J. Chem. Phys. 102 (1995) 5451–5459.
[106] A.E. Torda, R.M. Scheek, W.F. van Gunsteren, Time-dependent distance restraints in molecular-dynamics simulations, Chem. Phys. Lett. 157 (1989) 289–294.
[107] K. Matsuzaki, O. Murase, N. Fugii, K. Miyajima, An antimicrobial peptide, Magainin 2, induced rapid flip-flop of phospholipids coupled with pore formation and peptide translocation, Biochemistry 35 (1996) 11361–11368.
[108] L. Zhang, A. Rozek, R.E.W. Hancock, Interaction of cationic antimicrobial peptides with model membranes, J. Biol. Chem. 276 (2001) 35714–35722.
[109] M.L. Bodner, C.M. Gabrys, P.D. Parkanzky, J. Yang, C.A. Duskin, D.P. Weliky, Temperature dependence and resonance assignment of 13C NMR spectra of selectively and uniformly labeled fusion peptides associated with membranes, Magn. Reson. Chem. 42 (2004) 187–194.
[110] W. Qiang, J. Yang, D.P. Weliky, Solid-state nuclear magnetic resonance measurements of HIV fusion peptide to lipid distances reveal the intimate contact of beta strand peptide with membranes and the proximity of the Ala-14–Gly-16 region with lipid headgroups, Biochemistry 46 (2007) 4997–5008.
[111] C.M. Wasniewski, P.D. Parkanzky, M.L. Bodner, D.P. Weliky, Solid-state nuclear magnetic resonance studies of HIV and influenza fusion peptide orientations in membrane bilayers using stacked glass plate samples, Chem. Phys. Lipids 132 (2004) 89–100.
[112] J. Yang, C.M. Gabrys, D.P. Weliky, Solid-state nuclear magnetic resonance evidence for an extended beta strand conformation of the membrane-bound HIV-1 fusion peptide, Biochemistry 40 (2001) 8126–8137.
[113] J. Yang, P.D. Parkanzky, M.L. Bodner, C.A. Duskin, D.P. Weliky, Application of REDOR subtraction for filtered MAS observation of labeled backbone carbons of membrane-bound fusion peptides, J. Magn. Reson. 159 (2002) 101–110.

[114] J. Yang, P.D. Parkanzky, B.A. Khunte, C.G. Canlas, R. Yang, C.M. Gabrys, D.P. Weliky, Solid state NMR measurements of conformation and conformational distributions in the membrane-bound HIV-1 fusion peptide, J. Mol. Graph. Model 19 (2001) 129–135.
[115] J. Yang, M. Prorok, F.J. Castellino, D.P. Weliky, Oligomeric beta-structure of the membrane-bound HIV-1 fusion peptide formed from soluble monomers, Biophys. J. 87 (2004) 1951–1963.
[116] J. Yang, D.P. Weliky, Solid-state nuclear magnetic resonance evidence for parallel and antiparallel strand arrangements in the membrane-associated HIV-1 fusion peptide, Biochemistry 42 (2003) 11879–11890.
[117] R. Yang, M. Prorok, F.J. Castellino, D.P. Weliky, A trimeric HIV-1 fusion peptide construct which does not self-associate in aqueous solution and which has 15-fold higher membrane fusion rate, J. Am. Chem. Soc. 126 (2004) 14722–14723.
[118] R. Yang, J. Yang, D.P. Weliky, Synthesis, enhanced fusogenicity, and solid state NMR measurements of cross-linked HIV-1 fusion peptides, Biochemistry 42 (2003) 3527–3535.
[119] Z. Zheng, R. Yang, M.L. Bodner, D.P. Weliky, Conformational flexibility and strand arrangements of the membrane-associated HIV fusion peptide trimer probed by solid-state NMR spectroscopy, Biochemistry 45 (2006) 12960–12975.
[120] M. Hong, Oligomeric structure, dynamics, and orientation of membrane proteins from solid-state NMR, Structure 14 (2006) 1731–1740.
[121] W. Luo, M. Hong, Determination of the oligomeric number and intermolecular distances of membrane protein assemblies by anisotropic 1H-driven spin diffusion NMR spectroscopy, J. Am. Chem. Soc. 128 (2006) 7242–7251.